# Lateglacial to Holocene relative sea-level changes in the Stykkishólmur area, northern Snæfellsnes, Iceland

Martin D. Brader[1*], Jeremy M. Lloyd[1], Michael J. Bentley[1] and Anthony J. Newton[2]

[1]Department of Geography, University of Durham, Durham, UK
[2]School of GeoSciences, Institute of Geography and the Lived Environment, University of Edinburgh, UK

***Corresponding Author:** Martin D. Brader (m.d.brader@durham.ac.uk)

**Abstract:**

Comparatively little research has been undertaken on relative sea-level (RSL) change in western Iceland. This paper presents the results of diatom, tephrochronological and radiocarbon analyses on six isolation basins and two coastal lowland sediment cores from the Stykkishólmur area, northern Snæfellsnes, western Iceland. The analyses provide a reconstruction of Lateglacial to mid-Holocene relative sea-level changes in the region. The marine limit is measured to 65-69 m above sea level (asl), with formation being estimated at 13.5 cal ka BP. Relative sea-level fall initially occurred rapidly following marine limit formation, until *c.* 12.6 cal ka BP, when the rate of RSL fall decreased. RSL fell below present in the Stykkishólmur area during the early Holocene (by *c.* 10 cal ka BP). The rates of RSL change noted in the Stykkishólmur area demonstrate lesser ice thicknesses in Snæfellsnes than Vestfirðir during the Younger Dryas, when viewed in the regional context. Consequently, the data provide an insight into patterns of glacio-isostatic adjustment surrounding Breiðafjörður, a hypothesised major ice stream at the Last Glacial Maximum.

**Keywords:** sea-level, Iceland, isolation basin, diatom, reconstruction

## Introduction

During the Last Glacial Maximum (LGM), Iceland was covered by a considerable ice mass (Ingólfsson et al., 2010). However, in comparison to the UK and Fennoscandia, the extent and configuration of the LGM Icelandic Ice Sheet (IIS) is still relatively poorly understood, particularly in the Northwest (Andrews and Helgadóttir, 2003). Determining the scale of the LGM IIS is important, as freshwater input to the North Atlantic during deglaciation could have affected global thermohaline circulation (Hubbard et al., 2006). Consequently, various techniques have been employed to reconstruct the LGM IIS, including submerged feature mapping (e.g. Ólafsdóttir, 1975, Spagnolo and Clark, 2009), glacial striation identification (e.g. Keith and Jones, 1935, Hoppe, 1982), sedimentology (e.g. Andrews et al., 2000), ice sheet modelling (Hubbard et al., 2006) and ice stream investigation (e.g. Bourgeois et al., 2000). In addition, relative sea-level (RSL) studies have been employed to determine the patterns of deglaciation in Iceland, both through marine limit and geomorphological mapping (e.g. Ingólfsson, 1991; Norðdahl and Pétursson, 2005) and isolation basin study

(e.g. Rundgren et al., 1997). Despite this range of approaches, there remains uncertainty surrounding the vertical and lateral extent of the LGM IIS (Rundgren and Ingólfsson, 1999) and the associated style and pattern of deglaciation (Norðdahl *et al*., 2008).

One important area for LGM IIS investigations is Breiðafjörður, a large fjord separating Vestfirðir and Snæfellsnes (Fig. 1), as it was potentially the location of a major ice stream (Bourgeois et al., 2000, Hubbard et al., 2006). Previous research has investigated a number of features within the region, highlighting the potential maximum ice sheet extent at the LGM (e.g. Ólafsdóttir, 1975), former ice flow dynamics (Bourgeois et al., 2000) and marine limit elevations (e.g. Norðdahl and Pétursson, 2005, Fig. 1). The study of RSL on the northern coastline of Breiðafjörður has also provided an accurate age for deglaciation, alongside the rates of associated glacio-isostatic adjustment over the Lateglacial and Holocene (Lloyd et al., 2009, Fig. 1).

In this paper, we present the results of RSL study from Snæfellsnes, on the southern coast of Breiðafjörður, with the aim of reconstructing postglacial RSL change in order to investigate deglaciation and ice loading patterns through comparison with existing datasets. Six isolation basins and two coastal lowland cores were investigated, alongside mapping of the local marine limit, to produce a record of postglacial RSL change. This record provides an opportunity to determine rates of glacio-isostatic adjustment for comparison with Bjarkarlundur, situated 60 km north-northeast on the northern coast of Breiðafjörður (Lloyd et al., 2009).

**Previous Research**

As a result of limited empirical evidence of LGM IIS extent, ice-sheet modelling studies have been reliant upon a low number of dated raised shoreline and marine limit sites and a suite of undated marine-limit elevations (e.g. Le Breton et al., 2010). The marine-limit elevation, or highest point reached by postglacial sea level (Andrews, 1970), is linked to the timing of deglaciation at particular locations. It is therefore important to establish the age of marine limit formation, providing an opportunity to predict ice thickness and extent, when integrated into glacio-isostatic adjustment (GIA) models. Unfortunately, marine limit and raised shoreline sites often suffer from a lack of dateable material (e.g. (Principato, 2008) and poor spatial coverage, as well as having difficulties in relating the feature formation to mean sea-level (msl) (Lloyd et al., 2009). Despite this, several existing RSL and deglacial records have been developed using geomorphological evidence Norðdahl and Pétursson, 2005; Norðdahl *et al*., 2008).

Previous research has highlighted the spatial variability of marine limit and raised shoreline elevations in western Iceland (e.g. Hjort et al., 1985, Hansom and Briggs, 1991, Ingólfsson, 1991, Norðdahl and Asbjornsdottir, 1995, Norðdahl and Pétursson, 2005). The postglacial marine limit in Breiðafjörður ranges from 80 m asl in Bjarkarlundur (Lloyd et al., 2009) and 110 m asl in inner Breiðafjörður (Norðdahl and Pétursson, 2005, Fig. 1). A small number of

these locations have been dated (e.g. Norðdahl and Pétursson, 2005). In addition to the studies of highest postglacial RSL, previous research has also highlighted a period of low RSL at c. 10.2 – 10.6k cal a BP in western Iceland (Thors and Helgadóttir, 1991,Ingólfsson *et al*., 1995, Norðdahl and Pétursson, 2005). Submerged peats at -17 to -30 m asl have demonstrated a minimum position of postglacial RSL in western Iceland (T hors and Helgadóttir, 1991, Ingólfsson et al., 1995) and submerged terraces have demonstrated low points of -40 m (Norðdahl and Pétursson, 2005).

Isolation basin sediments have been widely used to construct comprehensive postglacial RSL records for a number of locations, including Norway (Kjemperud, 1986), Russia (Corner et al., 2001), the UK (Shennan et al., 2000) and Greenland (Long et al., 1999).Isolation basin studies have also been previously undertaken in Iceland (e.g. Rundgren et al., 1997, Lloyd et al., 2009). These RSL records can act as important tests for models of glacio-isostatic adjustment, providing an opportunity to investigate rates of isostatic uplift or subsidence over time. The first isolation basin study in Iceland was undertaken in northernmost Skagi (Fig. 1), demonstrating a total fall in RSL of 45 m at an average rate of -15.5 mm cal $a^{-1}$ between c. 13.2k cal a BP and c. 10.3k cal a BP, during which two transgressions of 5 m amplitude occurred (Rundgren et al., 1997). These transgressions have been linked to expansions of the IIS during the Younger Dryas and Preboreal (Rundgren et al., 1997; Norðdahl and Pétursson, 2005).

In Bjarkarlundur, Vestfirðir, a fall in RSL of ~80 m since deglaciation has been demonstrated (Lloyd et al., 2009). The research highlights two periods of rapid RSL change, with a rate of -38 mm cal $a^{-1}$ during the Bølling-Allerød and -16 mm cal $a^{-1}$ during the early Holocene (Lloyd et al., 2009). It was noted that the Younger Dryas reduced the rate of RSL fall in southern Vestfirðir to -4 mm cal $a^{-1}$ (Lloyd et al., 2009). In Bjarkarlundur, RSL fell below present around 9 cal ka BP, which correlates with the isolation basin record from Skagi (Rundgren et al., 1997) alongside records generated by other sources (Norðdahl and Pétursson, 2005). This fall below present at Bjarkarlundur was followed by a transgression during the late Holocene from which RSL is assumed to fall to present (Lloyd et al., 2009).

Furthermore, RSL study in western Iceland has demonstrated a series of raised shoreline features from the marine limit to close to present sea-level (Ingólfsson, 1988; Ingólfsson and Norðdahl, 2001; Norðdahl and Pétursson, 2005; Norðdahl et al., 2008; Ingólfsson et al., 2010). Ingólfsson and Norðdahl (2001) report marine limit shorelines at 105 m and 148 m asl in Akrafjall and Stóri-Sandhóll, Borgarfjörður, western Iceland, with Stóri-Sandhóll dating to c. 15.45 ± 0.245k cal a BP (uncorrected). A second extensive Younger Dryas shoreline is reported at 60 – 70 m asl (Ingólfsson and Norðdahl, 2001). The high marine limit elevations in the Borgarfjörður region are taken as a consequence of rapid deglaciation in western Iceland (Ingólfsson and Norðdahl, 2001).

**Research Location**

Snæfellsnes is a large peninsula in western Iceland, forming the southern coastline of Breiðafjörður (Fig. 1 and 2). Snæfellsnes is dominated by the ice-capped Snæfellsjökull volcanic system, which is situated to the extreme west of the peninsula. The geology of the area is characterised by the Snæfellsnes Volcanic Belt (SVB) which overlies Tertiary basalts and trends from east to west, contrasting with the typical north-south trend of the central volcanic zones (Sigurdsson, 1970). The region is classified as tectonically inactive, despite a number of small magnitude seismic events between 1912 and 1962 (Sigurdsson, 1970).

**Methodology**

This research employs a combination of bio- and lithostratigraphic data to investigate RSL changes using a range of field and laboratory methods. The key technique employed in this research is the isolation basin methodology (Kjemperud, 1986). Isolation basins are rock depressions, which have over time been inundated by and isolated from marine conditions (Lloyd et al., 2009), denoted by an isolation contact within the sediments. Kjemperud (1986) notes three isolation contacts within isolation basins: sedimentological, hydrological and diatomological. An accurate record of environmental change is preserved due to the impervious rock 'sill' (Lloyd and Evans, 2002), the altitude of which must be accurately measured, as it is the point which controls the dominant environmental conditions (marine, brackish or freshwater) at each site.

Potential isolation basin sites for analysis were identified in the field using the characteristics outlined by Long et al. (2011). Initial site stratigraphies were determined by coring transects using a gouge corer, with samples for analysis retrieved using a Russian or Livingstone corer depending on the site stratigraphy. Sediments were extracted from an infilled section of the basin or from the rear of a small boat where the lake covered the majority of the basin. Sediments were described using the Troëls-Smith (1955) classification scheme.

Samples were prepared for diatom analysis using the standard techniques outlined by Palmer and Abbott (1986). A minimum of 250 diatoms were enumerated per sample, using a range of taxonomic guides for identification (e.g. Brun, 1965, Foged, 1972, Foged, 1973, Foged, 1977, Hartley, 1996). Following identification, diatoms were grouped into five classes: marine, brackish, salt tolerant, freshwater and salt intolerant (Hustedt, 1957). Within this paper, summary diagrams are provided for each site, with full diatom counts available as supplementary information.

In order to determine the elevation of former RSL, the indicative meaning should be subtracted from the sill altitude (see Shennan et al., 1999). The indicative meaning is defined as the relationship between the dated sea-level index point and the tidal frame (van der Plassche, 1986), which was determined by combined bio- and lithostratigraphic analysis at each location to identify the hydro- and diatomological isolation contacts (Kjemperud, 1986). Mean High Water Spring Tide (MHWST) is frequently used for the diatomological

isolation contact (Lloyd et al., 2009; Long et al., 2011), which is characterised by predominantly freshwater conditions with a minor brackish element (Shennan et al., 1982; 1994). The hydrological isolation contact represents entirely freshwater conditions and equates to Highest Astronomical Tide (HAT; Shennan et al., 1982; 1994).

Tephrochronology and radiocarbon dating were employed to provide chronological control for the diatomological isolation contacts. The major element composition of tephra layers was determined by Wavelength Dispersive Analyses on a five spectrometer Cameca SX100 electron microprobe (EPMA) at the Tephra Analytical Unit, University of Edinburgh. Tephra samples were subjected to an acid digestion prior to analysis (Persson, 1971) and were subsequently sieved at 63 µm and 125 µm (e.g. Larsen et al., 1999). Tephra results were compared to previously published compositions using *Tephrabase* to identify individual horizons (Newton, 1996, Newton et al., 2007). Radiocarbon samples were generated as AMS bulk dates from organic sediments close to the diatomological isolation contact, following the standard preparation techniques. Radiocarbon ages were subsequently calibrated using CALIB 7.0 (Stuiver et al., 2005) and the IntCal13 calibration dataset (Reimer et al., 2013).

**Results**

Sites were selected at a range of altitudes from present sea level to the marine limit in order to investigate RSL changes throughout the Lateglacial and Holocene. Samples were collected from a small geographical area in order to minimise the impacts of differential rates of isostatic rebound (Fig. 2). Radiocarbon analyses at each site are summarised in Table 1 as 2σ ranges, with tephra geochemistries presented in supplementary information.

*Borgarland 10 (65° 2'40.78"N, 22°43'35.51"W) Core elevation: +1.8 m asl*

Borgarland is an extensive coastal lowland area grading into a modern saltmarsh to the north of Helgafell on the Thorsnes peninsula (Fig. 2). The lowland contains a former natural channel and later man-made drainage system. A total of 18 diatom samples were analysed, showing a transition from predominantly brackish to mainly freshwater conditions, with a minor brackish component towards the top of the core (Fig. 3a; Appendix 1). The diatomological isolation contact at 50 cm yields a radiocarbon age for the decrease in marine influence of 7156-7252 cal a BP.

*Borgarland 11 (65° 2'40.78"N, 22°43'35.51"W) Core elevation: +3.1 m asl*

A second core, Borgarland 11, was taken close to the location of Borgarland 10 (Fig. 2; Appendix 1). Four diatoms samples were counted to a minimum of 250 diatoms, but preservation was generally poor (Fig. 3). There were no visible tephra deposits within the sediment core. The diatom flora indicate a brackish-marine signal from the base of the core up to 104 cm (Fig. 3b). A radiocarbon date from 104 cm dates the transition from brackish to fully freshwater conditions to 9915–10097 cal BP.

*Skjaldarvatn (65°2'50.67"N, 22°47'11.35"W) Sill altitude: +4.6 m asl*

Skjaldarvatn is located to the SW of the Thorsnes peninsula (Fig. 2). The basin is elongated, 700 m long and 180 m wide and has an infilled section to the northeast of Skjaldarvatn lake. Higher ground is found to the north, south and east, with a stream draining the lake to the southwest. The bedrock sill was located within the stream bed, lying at +4.57 m asl. The sample for analysis was retrieved from the infilled section to the northeast (Appendix 1). A tephra layer at 546 cm was analysed, but could not be geochemically matched to any previously published record. Diatom analysis demonstrates a transition from marine to brackish dominance, followed by freshwater and salt intolerant species dominance (Fig. 3c). The shift in diatom assemblage from marine-brackish to freshwater dominance at 540 cm represents the isolation contact and is radiocarbon dated to 11253-11619 cal a BP (Fig. 3c).

*Þingvallavatn (65°3'33.30"N, 22°42'43.16"W) Sill altitude: +5.3 m asl*

Þingvallavatn is a basin situated to the north of the Thorsnes peninsula (TH1, Fig. 2). The basin contains a lake of approximately 300 m diameter, with the basin sill being covered by peat, situated to the northeast. A grid of cores led to the sill being identified at +5.34 m asl. Two transects were cored using a boat, with a sample for analysis being collected near to the centre of the lake (Appendix 1). The tephra layers at 456 cm and 479 cm were both analysed, providing chemical signatures which could not be matched to published data. Diatom analyses (Fig. 3d) revealed a basal marine-brackish zone, moving to a transitional brackish phase at 505-498 cm which is then replaced by freshwater conditions. The diatomological isolation contact is at 507 cm, providing a date for isolation of 11089-11219 cal a BP.

*Saurar 1 (65°1'4.53"N, 22°41'47.11"W) Sill altitude: +9.0 m asl*

The Saurar 1 basin is approximately 7 km south of Stykkishólmur (SA1, Fig. 2). Saurar 1 is situated within an area of low, undulating topography and is dissected by a forest road. The basin measures approximately 350 m long by 120 m wide, with an outlet stream draining the site to the northwest. The basin sill was identified based on a grid of cores and a sample was retrieved from the centre of the site (Appendix 1). Tephra analysis was undertaken on one sample from 334 cm, which demonstrated a mixed geochemical signature. Diatom analysis identifies a predominantly freshwater flora throughout the core, but with a significant marine-brackish component to the flora towards the base of the core. The diatomological isolation contact is at 332 cm, which was radiocarbon dated to 12135-12544 cal a BP (Fig. 3e).

*Helgafellsvatn (65°2'18.87"N, 22°44'23.25"W) Sill altitude: +12.8 m asl*

Helgafellsvatn is situated below Helgafell, a small hill of 60 m, which dominates the local landscape (HE1, Fig 2). The basin consists of a lake approximately 750 m long and 400 m wide, as well as an extensive infilled section to the northeast. The basin sill was located

close to the church at Helgafell. A transect of cores were taken from the infilled section at the lake edge, with a sample for analysis being extracted close to the centre of the transect (Appendix 1). The tephra layers at 578 cm and 615 cm are geochemically similar in composition but could not be identified and therefore were unable to assist in the constraint of isolation. Diatom analysis shows a lower marine-brackish zone (660-635 cm), an intermediate transitional zone (635-616 cm) and an upper freshwater zone (616-560 cm). The diatomological isolation contact at 616 cm was radiocarbon dated providing an age of 11224-11408 cal a BP (Fig. 3f).

*Saurar 3 (65°0'18.79"N, 22°43'6.19"W) Sill altitude: +16.2 m asl*

The basin at Saurar 3 is located along the same forest road as Saurar 1 (Fig. 2). The basin is made up of a large lake and bog, with the basin measuring 570 m by 180 m. Higher ground is found to the north, west and east, with a lower lying area to the south. The basin sill was identified through a coring grid to the south of the lake. A transect of cores was investigated to the north of the lake. A sample for analysis was collected using a Livingstone corer towards the centre of the core transect (Appendix 1). Geochemical analysis was undertaken on the two tephra layers. The upper tephra layer at 755 cm had a distinct Veiðivötn-type signature, with the lower deposit at 790 cm likely being sourced from Grímsvötn. Diatom analysis identified a transition from a basal marine-brackish zone (845-825 cm), to a brackish zone (825-810 cm) then an upper freshwater zone from 810 cm. A radiocarbon date from the diatomological isolation contact at 808 cm provided a calibrated age of 12558-12646 cal a BP (Fig. 3g).

*Ytra-Bárvatn (64°59'2.97"N, 23°11'39.34"W) Sill altitude: +57.6 m asl*

Ytra-Bárvatn is located on the Setberg peninsula approximately 20 km west of Stykkishólmur, and consists of a large lake with a diameter of approximately 220 m (YBR1, Fig. 2). The lake is drained to the west by a small stream, with the sill being identified within the stream bed. Higher ground is found to the north and south, with the basin situated within a small valley. The basin is situated below the highest raised shoreline identified in the area and thus provides a minimum age for highest postglacial sea-level. Two perpendicular transects were cored within the basin to establish site stratigraphy, with a sample being taken from the northern part of the lake, which yielded thicker sediments (Appendix 1). Within the core sample, two distinct tephra horizons at 210 cm and 354 cm underwent geochemical analysis. The upper tephra deposit did not have a homogeneous geochemical signature, being of mixed origin. However, the lower tephra deposit demonstrates a correlation with the Saksunarvatn tephra, providing an age of 10210 ± 35 cal a BP (Lohne et al, 2014; Fig. 4). A radiocarbon date from the diatomological isolation contact at 468 cm returned a calibrated age of 20074-20536 cal a BP Fig. 3h). A second date at 440 cm returned an age of ~24000 cal a BP, suggesting a problem with contamination at the site.

## Discussion

*Marine limit formation in northern Snæfellsnes*

In the Stykkishólmur area, the highest raised shorelines were measured between 65 m (BR1) and 69 m (OS1) asl (Fig. 2). These local marine limit values are lower than postglacial marine limits identified on the northern shore of Breiðafjörður at 78 m-98 m (Lloyd et al., 2009) and those identified in inner Breiðafjörður at 90 m-110 m (Norðdahl and Pétursson, 2005). However, the marine limit elevation identified in the Stykkishólmur area is similar to the altitude of the postglacial marine limit from Skagi at 65 m (Rundgren et al., 1997) and elsewhere in western Iceland at 60 m-70 m (Ingólfsson, 1991), which formed during the Bölling Period (Norðdahl and Pétursson, 2005). In addition, the marine limit lies at a similar elevation to the Younger Dryas marine limit identified in innermost Breiðafjörður (Norðdahl and Asbjornsdottir, 1995). Consequently, if the Stykkishólmur area marine limit is to be used to assess glacio-isostatic adjustment in the region, detailed chronological control of the marine limit is needed, as marine limits of similar elevation appear not to have all formed simultaneously.

Isolation basin studies provide an opportunity to determine the age of the marine limit at a given location and also the minimum age for deglaciation where sites with elevations close to the marine limit are available (e.g. Lloyd et al., 2009). Ytra-Bárvatn, the highest basin investigated in this study, at 57.6 ± 0.6 m asl could therefore provide a minimum date for deglaciation in northern Snæfellsnes. The diatom assemblage of Ytra-Bárvatn demonstrates a weak brackish signal towards the base of the core sample (Fig. 3h). This most likely indicates a weak marine signal, as the basin is close to isolation and therefore only inundated for part of the tidal cycle.

Three radiocarbon dates were obtained at Ytra-Bárvatn in order to establish the timing of the decrease in marine influence at the site and establish the age of tephra deposits found in the sediment sample retrieved. The lowest bulk sediment sample at 468 cm provided an age of 16841 ± 76 $^{14}$C a BP (20074-20536 cal a BP), which is considerably older than previously reported isolation basin records (e.g. Rundgren *et al*., 1997; Lloyd *et al*., 2009). This sample was organic-poor and it is therefore likely that the age generated is misrepresentative of the basin isolation, being affected by the in-washing of carbon from the surrounding landscape (Björck and Wohlfarth, 2001) or reservoir effects. Björck and Wohlfarth (2001) have demonstrated that similar organic-poor sediments have produced dates which are thousands of years older than organic-rich sediments in similar settings. Previous research has highlighted that plant macrofossils provide the most reliable dating constraints from lake sediments (Abbott and Stafford Jr, 1996) however, the lack of identifiable plant macrofossils within the isolation basin sediments led to the use of bulk AMS dates in this study. Similar limitations have been highlighted in other isolation basin records in Iceland (e.g. Lloyd et al. (2009).

Consequently, the date produced from the commencement of organic sedimentation at the site may be more representative of basin isolation, once the position within the tidal frame represented has been established. However, a second date at 440 cm provided an even older age (Table 1), suggesting a problem with old carbon contamination at the site. The upper tephra deposits within the Ytra-Bárvatn sediment sample were of mixed geochemistry and therefore likely represent the reworking of tephra from the surrounding landscape. The geochemical analysis of the lower tephra deposit at YBR1, however, demonstrates a good correlation to the Saksunarvatn tephra (Fig. 4). Using this as a chronological marker (10210 ± 35 cal a BP; Lohne et al., 2014) and assuming constant sedimentation throughout the core sample, it is possible to estimate the timing of isolation at the site, if all radiocarbon ages are discounted (due to potential contamination). If these two assumptions are accepted, basin isolation can be estimated to c. 13500 cal a BP. Indeed this is likely to be a minimum age, as the rate of sedimentation is likely to be relatively lower initially after isolation of the basin (relatively organic poor accumulation), rising slightly as organic content increases.

Extrapolation using the sedimentation rate between the upper radiocarbon date at 210cm and Saksunarvatn tephra at 354 cm provides a younger age of isolation of c. 12.2 cal a BP which would correlate well with the Younger Dryas shorelines in inner Breiðafjörður ((Norðdahl and Asbjornsdottir, 1995). The full range of possible ages for isolation of Ytra-Bárvatn are, therefore, plotted on fig. 5. However, the younger extrapolated isolation age is younger than isolation ages of lower basins, such as SA1 and SA3. In order for this scenario to be accepted, both lower basins would need to be affected by contamination from older carbon within the landscape. Whilst this is possible, our preferred interpretation is for an age for the isolation of YBR1 of c. 13.5 cal. ka BP, which correlates well with the results of Lloyd et al. (2009).

Accordingly, we propose that the marine limit identified in the Stykkishólmur area formed prior to the Younger Dryas, supported by the radiocarbon ages retrieved from lower elevation sites. Previous studies in the Bjarkarlundur area (Lloyd et al., 2009), northernmost Skagi (Rundgren et al., 1997) and lower Borgarfjörður (Ingólfsson and Norðdahl 2001) have determined ages of 14125 ± 340 cal. a BP, >14000 cal. a BP and 15,450 ± 245 cal. a BP respectively for the marine limit shorelines in these areas. The estimated age of the marine limit in the Stykkishólmur area based on the isolation of Ytra-Bárvatn (> 13500 cal a BP), therefore, appears reasonable.

*Lateglacial to mid-Holocene RSL change*

The six isolation basin and two coastal lowland sites investigated in northern Snæfellsnes constrain the RSL change during the Lateglacial to mid-Holocene (Table 1, Fig. 6). Based on our preferred interpretation a new RSL curve for the Stykkishólmur area has been constructed using the isolation basin and coastal lowland sea-level index points (Fig. 6), with chronological control being provided through radiocarbon dates and tephra analysis.

Following deglaciation, RSL fell rapidly over the course of the Lateglacial and early Holocene in northern Snæfellsnes. Following the isolation of Ytra-Bárvatn (YBR1, 57.6 m asl RSL fall occurred rapidly until the isolation of Saurar 3 (SA3, 16.2 m asl) at 12544-12722 cal a BP (Fig. 6). This RSL fall demonstrates the rapid rate of isostatic rebound, which is comparable to regional trends (Lloyd *et al*., 2009). This correlation is likely given the relative proximity of the two study areas (~60km) (Fig. 1). The rates of initial RSL fall and isostatic rebound reported in Skagi (Rundgren et al., 1997) are notably lower than those reported for the Stykkishólmur and Bjarkarlundur areas (Lloyd et al., 2009).

Following the isolation of Saurar 3 (SA3, 16.2 m asl), the rate of RSL change decreased to -24.5 mm cal $a^{-1}$ until the isolation of Saurar 1 (SA1, 9.0 m asl) at 12135-12544 cal a BP. This reduced rate of RSL change corresponds to a decrease in the rate of isostatic rebound to +46 mm cal $a^{-1}$, when eustatic sea-level changes over the period are taking into consideration (Fairbanks, 1989). Previous studies have demonstrated a similar reduction in the rate of RSL change during this period, associated with the expansion of Younger Dryas ice caps and glaciers (Lloyd et al., 2009).

From the RSL record generated in this study, there is only evidence for a limited Younger Dryas ice readvance, as there is little indication of a notable transgression during this period in the Stykkishólmur area. The RSL curve generated for the Stykkishólmur area suggests an exponential decrease in the rate of glacio-isostatic rebound since deglaciation and thus minimal influence from Younger Dryas ice regrowth. It is also evident that RSL was higher on the northern coast of Breiðafjörður during this period (Lloyd et al., 2009) (Fig. 7). This difference in RSL could be attributed to a larger Younger Dryas ice cap in Vestfirðir than on the Snæfellsnes peninsula (Norðdahl and Pétursson, 2005).

Following the isolation of Saurar 1 (9.0 m asl), RSL fell to between 2.4 and 3.2 m asl, with a decrease in marine influence noted at Skjaldarvatn (SK1) between 11253-11619 cal a BP and the isolation of Þingvallavatn (TH1) at 11066-11241 cal a BP (Fig. 6). These decreases in marine influence likely occurred in quick succession, as the error associated with the determination of site elevation and decrease in marine influence mean that these events could have occurred concurrently. Both Skjaldarvatn and Þingvallavatn have visible tephra deposits close to the point of decreased marine influence.

Þingvallavatn shows a clear shift from marine-brackish to freshwater dominance within the diatom assemblage (Fig. 3d) and contains two tephra layers with geochemical signatures which are unable to be matched to previous records (Fig. 4). The geochemical signature attained from analysis of the Skjaldarvatn deposits shows a mixed assemblage, with tephra shards demonstrating Veiðivötn-, Grímsvötn- Katla- and SVB-type geochemical compositions (Tephrabase, 2012). It is possible that the geochemical signal highlighted in the Þingvallavatn core is masked at Skjaldarvatn by the in-washing of additional material from the surrounding landscape. A mixed tephra composition is likely the result of an

unvegetated landscape, where tephra can move freely without being trapped by plant material or sediment.

At Skjaldarvatn, the transition between marine-brackish and freshwater dominance is very sharp (Fig. 3c). This transition within the diatom assemblage is likely affected by the tephra deposit at 546 cm, however basin isolation had commenced prior to this point in the diatom assemblage. As a result, the age of isolation of Skjaldarvatn is older than anticipated due to the radiocarbon age being sought at the point of freshwater dominance rather than the completion of isolation within the diatom assemblage. However, there is relatively little influence on the RSL curve for the region.

It is clear that RSL was between 2.4 m and 3.2 m asl between 11066-11241 and 11253-11619 cal a BP when corrected for the indicative meaning. As a result, the timing of isolation at Helgafellsvatn appears to be anomalous (Figs. 5 and 6). The diatom assemblage for the site demonstrates a clear transition between marine-brackish and freshwater dominance suggesting a relatively rapid isolation of the basin (Fig. 3). However, the timing of isolation appears anomalously young compared to the other sites presented here (11224-11408 cal a BP). Based on our preferred interpretation the date from Helgafellsvatn must therefore be anomalous; hence, it is not used to constrain RSL. An alternative interpretation accepting the age of the isolation contact at Helgafellsvatn would require a rise in RSL of approximately 5 m following the isolation of SA1 at 12135-12544 cal a BP, or a larger rise of approximately 8 m following the isolation of SK1 at 11253-11619 cal a BP. An additional alternative interpretation is that the isolation contacts for sites SA3, SA1, SK1 and (to a lesser degree) TH1 are too old and the rate of RSL fall during the Lateglacial is rather more gradual than our preferred interpretation suggests.

*Mid- to Late Holocene RSL change*

Following the isolation of Þingvallavatn (TH1; 5.3 m asl) at 11066-11241 cal a BP, a sea-level index point at the coastal marsh site at Borgarland (BO11) records RSL falling below 0.9 m at 9915-10097 cal a BP (Fig. 6). Following this, RSL likely fell below present, the index point from BO10 records RSL below present (at -0.5 m) by 7148-7259 cal a BP (Fig. 6). This fall below present sea-level is later than existing records, which demonstrate a fall below present sea-level at *c.* 8.2 – 10.6 ka cal BP (Rundgren et al., 1997, Norðdahl and Pétursson, 2005, Lloyd et al., 2009). The RSL index point from BO10 suggests that RSL likely fell lower than this point during the mid-Holocene. Following this, there are two scenarios: a transgression during the mid-Holocene or a gradual rise to present.

The altitude of transgression during the mid-Holocene is limited by the lack of a second marine incursion recorded in the diatom assemblage from Skjaldarvatn or Þingvallavatn. As a result, RSL did not reach higher than 2.4 ± 0.7 m asl during the mid- to late Holocene in the Stykkishólmur area. There is however a short lived reoccurrence of mesohalobous species within the Borgarland sequence (Borgarland 10, Fig. 3a). Previous studies have noted the

potential for Holocene transgressions in Iceland, including in the northeast at c. 4 m asl at 7.3 cal ka BP (Richardson, 1997), southwest at 2-6 m asl at 2.9 and 2.3 cal ka BP (Simonarson and Leifsdóttir, 2002) and Hvammsfjörður, western Iceland at 3 m and 5 m asl after 4.5 cal. ka BP (Norðahl and Pétursson, 2005; Ingólfsson et al., 2010). In order to further develop the late Holocene RSL record for Snæfellsnes, additional sites at low elevations are required. However, such sites were not identified in the Stykkishólmur area and sites on the southern coast of the Snæfellsnes peninsula were determined to be unsuitable for isolation basin research due to the nature of the basin sills.

**Conclusions**

The study of RSL change in the Stykkishólmur area offers an opportunity to investigate GIA on the south coast of Breiðafjörður, when coupled with existing isolation basin and marine limit records from the region. The RSL record from the Stykkishólmur area highlights a difference in patterns of GIA in and around Breiðafjorður since deglaciation. In the Stykkishólmur area, the postglacial marine limit is identified at 63-69 m asl. Previous research has highlighted higher marine limit elevations in northern and innermost Breiðafjorður than determined in this study. This indicaties that ice thicknesses were likely greater in northern and innermost Breiðafjörður than in the Stykkishólmur area prior to deglaciation, or that deglaciation occurred later in the Stykkishólmur area.

Relative sea-level fell rapidly following deglaciation on both the northern (Lloyd et al., 2009) and southern coastlines of Breiðafjörður. The rate of RSL fall in the Stykkishólmur area correlates well with Lloyd et al. (2009) when the hypothesised marine limit age of 13500 cal. a BP is employed. The new RSL record from the Stykkishólmur area also provides an opportunity to explore the consequences of Younger Dryas ice regrowth. There is no evidence for a transgression during the Younger Dryas based on the isolation basin data from the Stykkishólmur area. Instead, the RSL curve shows a decrease in the rate of isostatic rebound from the LGM. There is little evidence for the influence of Younger Dryas ice regrowth in the Stykkishólmur area in the RSL record. This differs from the results on the northern coastline of Breiðafjörður (Lloyd et al., 2009), suggesting variation in ice conditions between the north and south coast of Breiðafjörður during the Younger Dryas, and that the influence of any glacial loading was relatively localised and did not significantly affect the Stykkishólmur area.

During the mid-Holocene, RSL fell below present at 7148-7259 cal. a BP following the decrease in marine influence at Borgarland 11 at 9915-10097 cal. a BP. This appears later than noted in previous studies in western Iceland, which have noted a RSL fall below present at ~8.2-10.6 cal ka BP (e.g. Lloyd et al., 2009). There is evidence of a subsequent minor transgression during the Late Holocene reaching less than 2.4 m asl (based on the indicative meaning correction of the sill elevation at Skjaldarvatn). Following this, RSL regressed to present although additional RSL data is required to better constrain these recent RSL changes.

**Acknowledgements**

This work was supported by the NERC Radiocarbon Facility NRCF010001 (Allocation Number 1689.0313) and the NERC Tephra Analytical Unit (Allocation Number TAU66/0511 and TAU78/1012) in the School of GeoSciences, University of Edinburgh. MDB was supported by a Van Mildert College Postgraduate Award. Assistance in the field was provided by Mateusz Strzelecki (2010) and Sam Gunter (2012). MDB would like to thank Andrew Dugmore, the University of Edinburgh and the North Atlantic Biocultural Organisation for vehicle support and Kate Smith for discussions of tephra geochemistry. We also thank the reviewers of this manuscript for their constructive comments.

**Abbreviations**. HAT, highest astronomical tide; IIS, Iceland Ice Sheet; LGM, Last Glacial Maximum; MHWST, mean high water spring tide; RSL, relative sea level.

**References**

Abbott MB, Stafford Jr TW. 1996. Radiocarbon geochemistry of modern and ancient Arctic lake systems, Baffin Island, Canada. *Quaternary Research* **45**: 300-311.

Andrews J, Helgadóttir G. 2003. Late Quaternary Ice Cap Extent and Deglaciation, Hunafloaáll, Northwest Iceland: Evidence from Marine Cores. *Arctic, Antarctic, and Alpine Research* **35**: 218-232.

Andrews JT, Hardardóttir J, Helgadóttir G, Jennings AE, Geirsdóttir Á, Sveinbjörnsdóttir ÁE, Schoolfield S, Kristjánsdóttir GB, Smith LM, Thors K, Syvitski J. 2000. The N and W Iceland Shelf: Insights into Last Glacial Maximum ice extent and deglaciation based on acoustic stratigraphy and basal radiocarbon AMS dates. *Quaternary Science Reviews* **19**: 619-631.

Björck S, Wohlfarth B 2001. 14C chronostratigraphic techniques in paleolimnology. *Tracking environmental change using lake sediments.* Springer.

Bourgeois O, Dauteuil O, Vliet-Lanoë BV. 2000. Geothermal control on flow patterns in the Last Glacial Maximum ice sheet of Iceland. *Earth Surface Processes and Landforms* **25**: 59-76.

Brun J. 1965. *Diatomées des Alpes et du jura,* Asher: Amsterdam.

Corner GD, Kolka VV, Yevzerov VY, Møller JJ. 2001. Postglacial relative sea-level change and stratigraphy of raised coastal basins on Kola Peninsula, northwest Russia. *Global and Planetary Change* **31**: 155-177.

Einarsson Þ. 1968. *Jarðfræði, saga bergs og lands (In Icelandic),* Mál og menning: Reykjavik.

Fairbanks RG. 1989. A 17,000-year glacio-eustatic sea-level record - influence of glacial melting rates on the Younger Dryas event and deep-ocean circulation. *Nature* **342**: 637-642.

Foged N. 1972. The diatoms in four postglacial deposits in Greenland. *Meddelelser om Grønland* **194**: 1-66.

Foged N. 1973. Diatoms from southwest Greenland. *Meddelelser om Grønland* **194**: 1-84.

Foged N. 1977. The diatoms of four postglacial deposits at Godthåbsfjord, west Greenland. *Meddelelser om Grønland* **199**: 1-64.

Hansom JD, Briggs DJ (eds.) 1991. *Sea-level changes in Vestfirðir, north west Iceland,* Dordrecht: Kluwer Academic.

Hartley B. 1996. *An atlas of British diatoms,* Biopress: Bristol.

Hjort C, Ingólfsson O, Norðdahl H. 1985. Late Quaternary geology and glacial history of Hornstrandir, northwest Iceland: a reconnaissance study. *Jokull* **35**: 9-29.

Hoppe G. 1982. The extent of the last inland ice sheet in Iceland. *Jökull* **32**: 3-11.

Hubbard A, Sugden D, Dugmore A, Norðdahl H, Pétursson HG. 2006. A modelling insight into the Icelandic Last Glacial Maximum ice sheet. *Quaternary Science Reviews* **25**: 2283-2296.

Hustedt F. 1957. Diatoméenflora der fluss-systems der weser im gebeit der Hansestadt Bremen. *Abhandlungen Herausgegeben von Naturwissenschaftlichen Verein zu Bremen* **34**: 181-440.

Ingólfsson Ó 1991. A Review of the Late Weichselian and Early Holocene Glacial and Environmental History of Iceland. *In:* Maizels J, Caseldine C (eds.) *Environmental Change in Iceland: Past and Present.* Springer Amsterdam.

Ingólfsson O, Norðdahl H, Haflidason H. 1995. Rapid isostatic rebound in southwestern Iceland at the end of the last glaciation. *Boreas* **24**: 245-259.

Ingólfsson Ó, Norðdahl H, Schomacker A 2010. 4 Deglaciation and Holocene Glacial History of Iceland. *In:* Anders Schomacker JK, Kurt HK (eds.) *Developments in Quaternary Sciences.* Elsevier: Amsterdam.

Keith DB, Jones EW. 1935. Grímsey, North Iceland. *Geographical Journal* **86**: 143-152.

Kjemperud A. 1986. Late Weichselian and Holocene shoreline displacement in the Trondheimsfjord area, central Norway. *Boreas* **15**: 61-82.

Larsen G, Dugmore A, Newton A. 1999. Geochemistry of historical-age silicic tephras in Iceland. *Holocene* **9**: 463-471.

Le Breton E, Dauteuil O, Biessy G. 2010. Post-glacial rebound of Iceland during the Holocene. *Journal of the Geological Society* **167**: 417-432.

Lloyd JM, Evans JR. 2002. Contemporary and fossil foraminifera from isolation basins in northwest Scotland. *Journal of Quaternary Science* **17**: 431-443.

Lloyd JM, Norðdahl H, Bentley MJ, Newton AJ, Tucker O, Zong YQ. 2009. Lateglacial to Holocene relative sea-level changes in the Bjarkarlundur area near Reykholar, North West Iceland. *Journal of Quaternary Science* **24**: 816-831.

Long AJ, Roberts DH, Wright MR. 1999. Isolation basin stratigraphy and Holocene relative sea-level change on Arveprinsen Ejland, Disko Bugt, West Greenland. *Journal of Quaternary Science* **14**: 323-345.

Long AJ, Woodroffe, S.A., Roberts, D.H., Dawson, S. 2011. Isolation basins, sea-level changes and the Holocene history of the Greenland Ice Sheet. *Quaternary Science Reviews* **30**: 3748-3768.

Newton AJ. 1996. Tephrabase: a tephrochronological database. *Quaternary Newsletter* **78**: 8-13.

Newton AJ, Dugmore AJ, Gittings BM. 2007. Tephrabase: tephrochronology and the development of a centralised European database. *Journal of Quaternary Science* **22**: 737-743.

Norðdahl H, Ásbjörnsdóttir L 1995. Isaldarlok i Hvammsfirdi. *In:* Hroarsson B, Jónsson D, Jónsson SS (eds.) *Eyjar i Eldhafi.* Got mal: Reykjavik.

Norðdahl H, Ingólfsson O, Pétursson HG. 2012. Deglaciation of Iceland and Relative Sea-level Changes. *Natturufraedingurinn* **82**: 73-86.

Norðdahl H, Pétursson HG (eds.) 2005. *Relative Sea-Level Changes in Iceland; new Aspects of the Weichselian Deglaciation of Iceland,* Amsterdam: Elsevier.

Ólafsdóttir Þ. 1975. Jökulgarður á sjávarbotni út af Breiðafirði (English summary: A moraine ridge on the Iceland shelf, west of Breiðafjördur). *Náttúrufræðingurinn* **45**: 247-271.

Palmer AJM, Abbott WH 1986. Diatoms as indicators of sea-level change. *In:* Van Der Plassche O (ed.) *Sea-Level Research: a manual for the collection and evaluation of data.* Geo Books: Norwich.

Persson C. 1971. Tephrochronological investigations of peat deposits in Scandinavia and on the Faroe Islands. *Sveriges Geologiska Undersokning Arbok* **65**: 1-34.

Principato SM. 2008. Geomorphic evidence for Holocene glacial advances and sea level fluctuations on eastern Vestfiroir, northwest Iceland. *Boreas* **37**: 132-145.

Reimer PJ, Bard E, Bayliss A, Beck JW, Blackwell PG, Bronk Ramsey C, Buck CE, Cheng H, Edwards RL, Friedrich M, Grootes PM, Guilderson TP, Haflidason H, Hajdas I, Hatté C, Heaton T, Hoffmann DL, Hogg AG, Hughen KA, Kaiser KF, Kromer B, Manning SW, Niu M, Reimer RW, Richards DA, Scott EM, Southon JR, Staff RA, Turney CSM, Van Der Plicht J. 2013. *IntCal13 and Marine13 Radiocarbon Age Calibration Curves 0–50,000 Years cal BP*.

Rundgren M, Ingólfsson Ó. 1999. Plant survival in Iceland during periods of glaciation? *Journal of Biogeography* **26**: 387-396.

Rundgren M, Ingólfsson O, Bjorck S, Jiang H, Hafliðason H. 1997. Dynamic sea-level change during the last deglaciation of northern Iceland. *Boreas* **26**: 201-215.

Shennan I, Lambeck K, Horton B, Innes J, Lloyd J, Mcarthur J, Purcell T, Rutherford M. 2000. Late Devensian and Holocene records of relative sea-level changes in northwest Scotland and their implications for glacio-hydro-isostatic modelling. *Quaternary Science Reviews* **19**: 1103-1135.

Shennan I, Tooley M, Green F, Innes J, Kennington K, Lloyd J, Rutherford M. 1999. Sea level, climate change and coastal evolution in Morar, northwest Scotland. *Geologie En Mijnbouw-Netherlands Journal of Geosciences* **77**: 247-262.

Sigurdsson H. 1970. Structural origin and plate tectonics of the snaefellsnes volcanic zone, Western Iceland. *Earth and Planetary Science Letters* **10**: 129-135.

Spagnolo M, Clark CD. 2009. A geomorphological overview of glacial landforms on the Icelandic continental shelf. *Journal of Maps* **5**: 37-52.

Stuiver M, Reimer PJ, Reimer RW. 2005. Calib 6.0 www program and associated documentation. *http://calib.qub.ac.uk/calib/*.

Tephrabase. 2012. *Tephrabase: a tephrochronological database* [Online]. Available: www.tephrabase.org [Accessed 03/06/14 2014].

Thors K, Helgadóttir G 1991. Evidence from south west Iceland of low sea level in early Flandrian times. *In:* Maizels JK, Caseldine C (eds.) *Environmental Change in Iceland: Past and Present.* Kluwer Academic Publishers: Dordrecht.

Troëls-Smith J. 1955. *Characterisation of unconsolidated sediments,* Danmarks Geologiske Undersøgelse: Copenhagen.

Van Der Plassche O. 1986. *Sea-level research: a manual for the collection and evaluation of data,* Geobooks: Norwich.

Figure 1: Map of northwest Iceland showing the marine limit elevation, submerged glacial features and relative sea-level studies within Breiðafjörður. The marine limit elevation is postglacial except for Area B, which has been dated to the Younger Dryas. The study site is Area C.

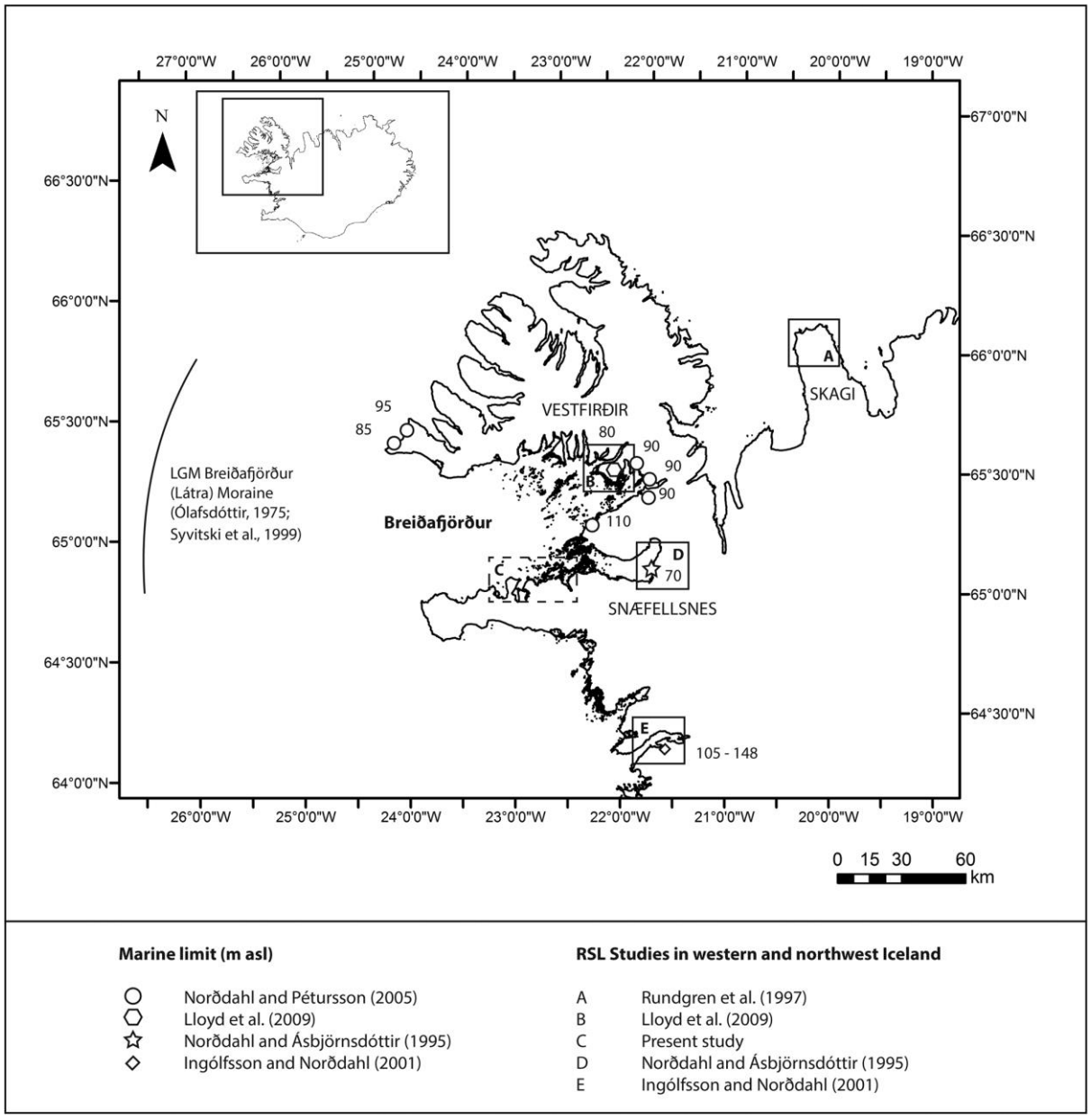

Figure 2: Location of isolation basins (SK1 – Skjaldarvatn, TH1 – Þingvallavatn, HE1 – Helgafellsvatn, SA1 - Saurar 1, SA3 – Saurar 3 and YBR1 – Ytra Bárvatn; grey circles) coastal lowland (BO10 – Borgarland 10 and BO11 – Borgarland 11; grey circle) and marine limit sites (OS1 – Ös and BR1 – Barar; black circles) in northern Snæfellsnes. Basemap is based on data from *National Land Survey of Iceland*.

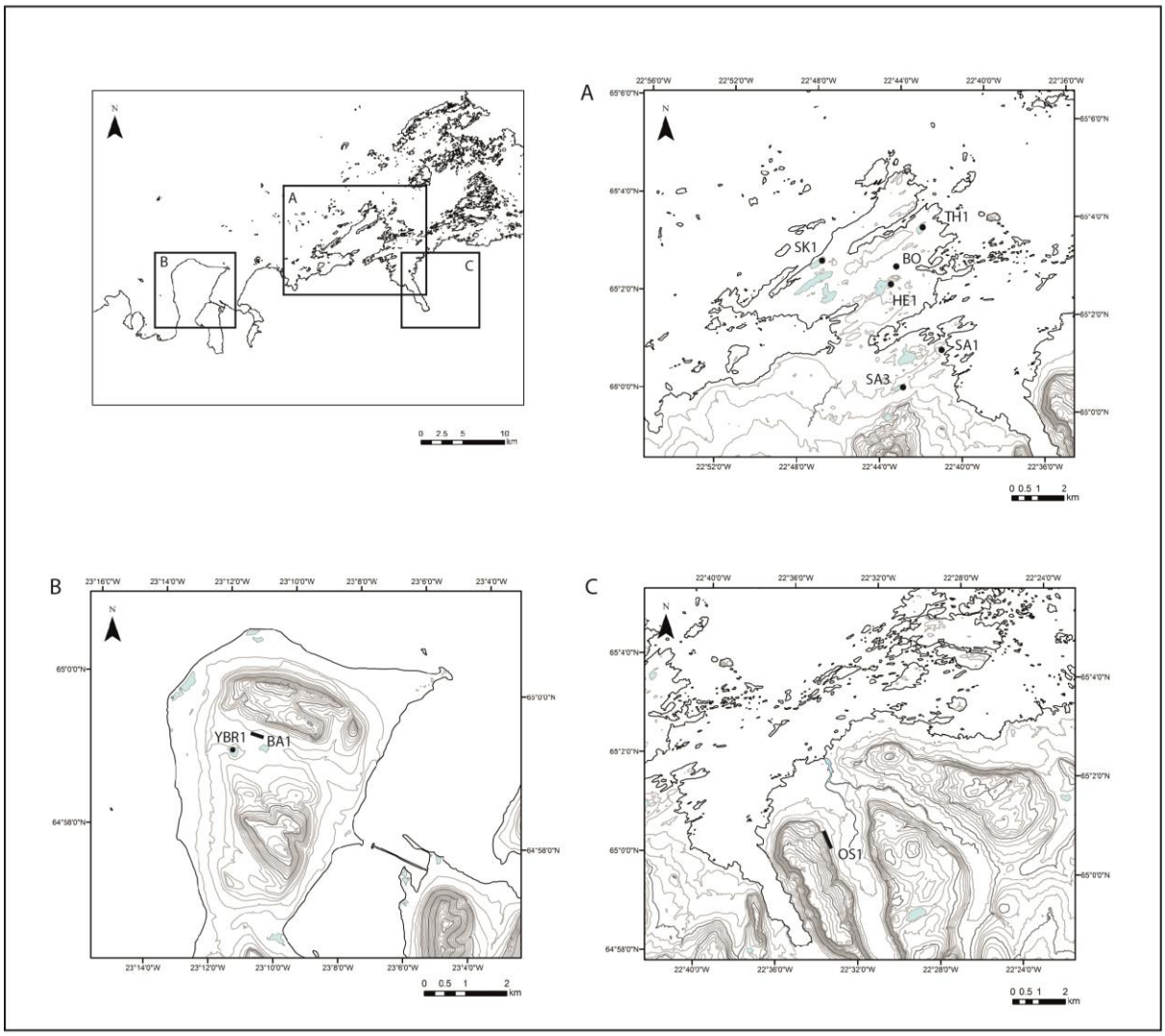

Figure 3: Summary diatom assemblages and lithostratigraphy from isolation basin and coastal lowland sites in Snæfellsnes. Full diatom diagrams are available from the corresponding author upon request. Calibrated ages are reported where appropriate. A: Borgarland 10, B: Borgarland 11, C: Skjaldarvatn, D: Þingvallavatn, E: Saurar 1, F: Helgafellsvatn, G: Saurar 3, H: Ytra-Bárvatn.

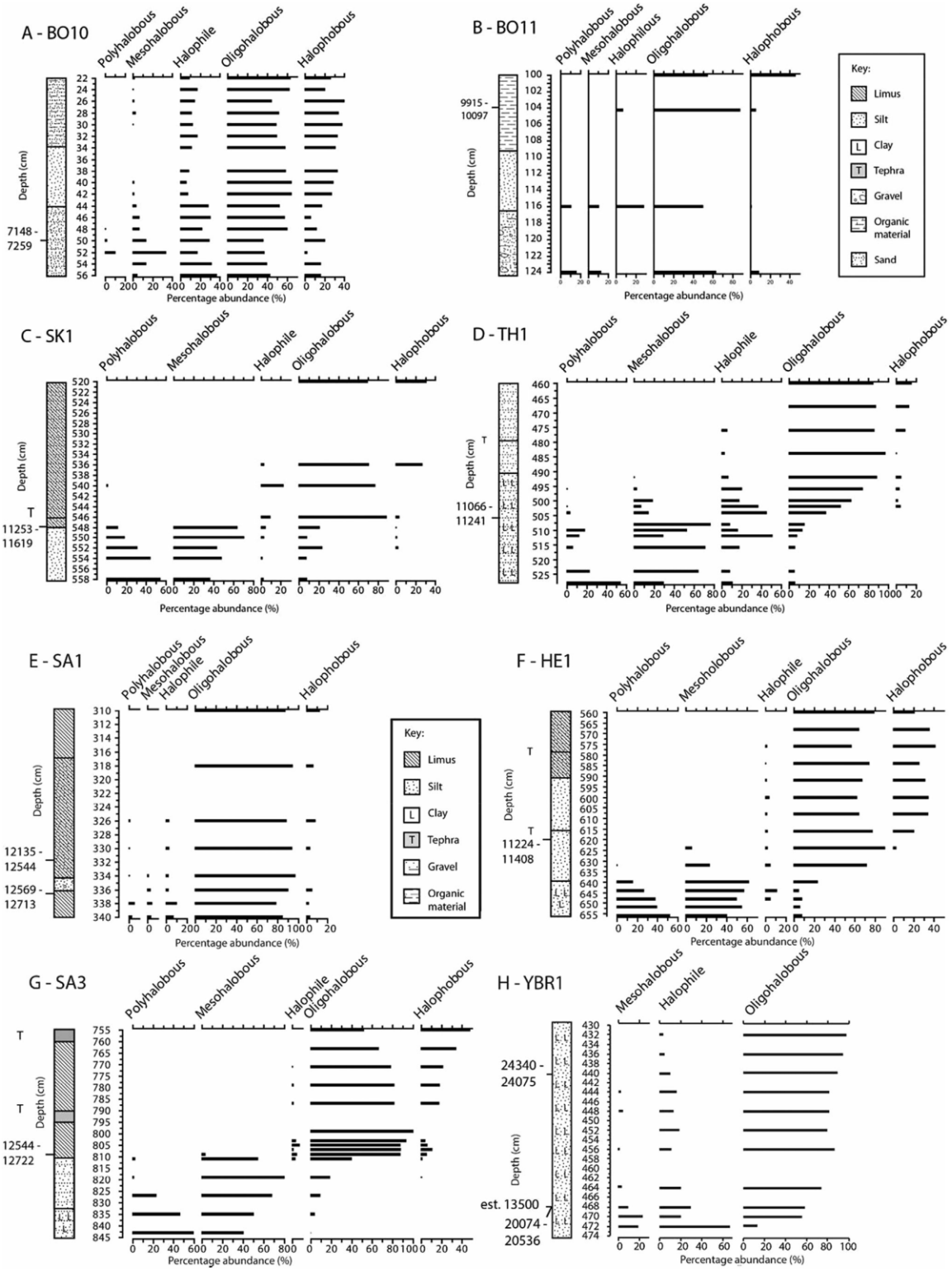

Figure 4: Tephra geochemistry for Ytra-Bárvatn, northern Snæfellsnes. Saksunarvatn data from *Tephrabase (www.tephrabase.org; Newton, 1996*). Analytical Conditions - Beam Voltage: 15kV; Beam Current: 2nA for Si, K, Al, Fe, Mg, Na, Ca and 80nA for Ti, Mn and P; Beam Size: 8 µm. A mixture of minerals, metals and artificial glasses were used to calibrate the instruments and analytical stability was checked using a BCR2G standard.

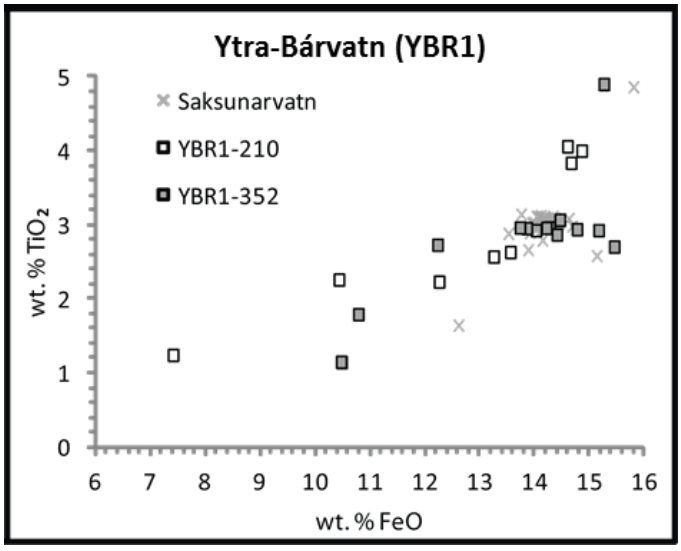


Figure 5: Age-depth profile for Ytra Bárvatn, showing the possible ages of isolation at the site.

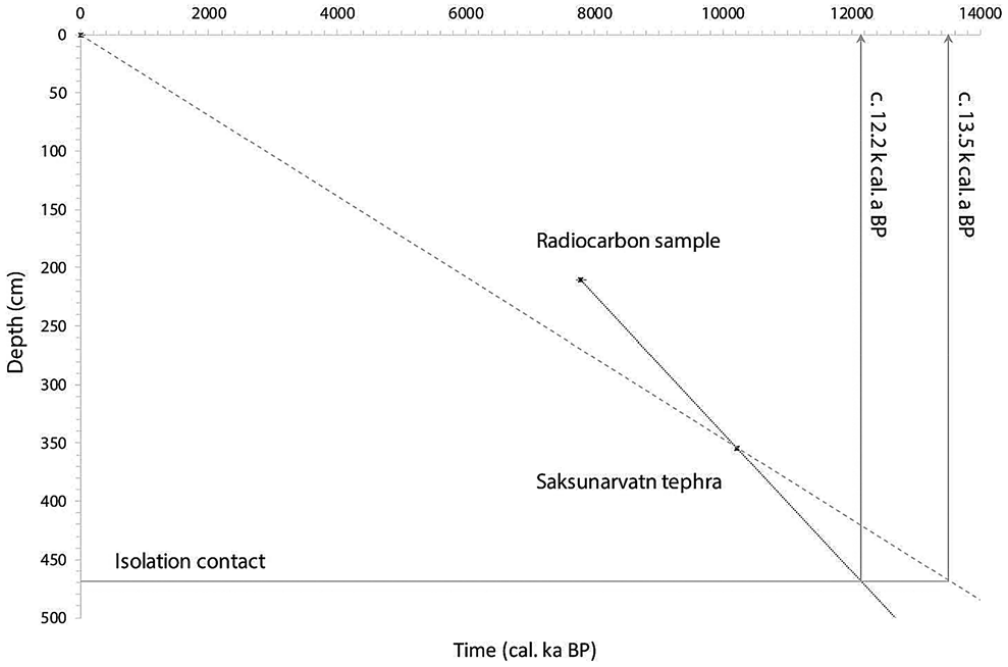

Figure 6: RSL curve for northern Snæfellsnes, with sea-level index points plotted against calibrated ages. Sea-level index point at HE1 is not used to constrain the curve due to a presumed incorrect age of isolation.

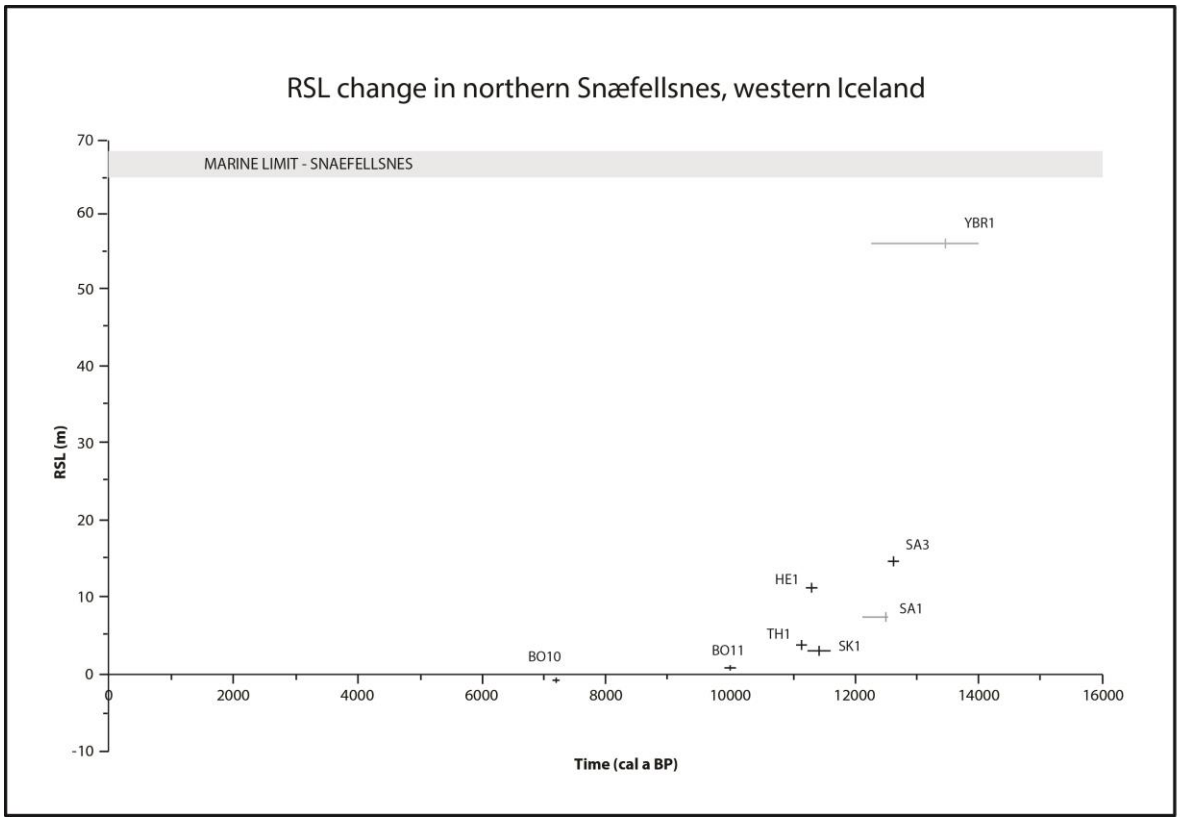

Figure 7: RSL curves from northwest Iceland, demonstrating regional trends and variability between sites investigated in Snæfellsnes (black, this study), Bjarkarlundur, Vestfirðir (red, Lloyd *et al*., 2009) and Skagi (blue, Rundgren *et al*., 1997).

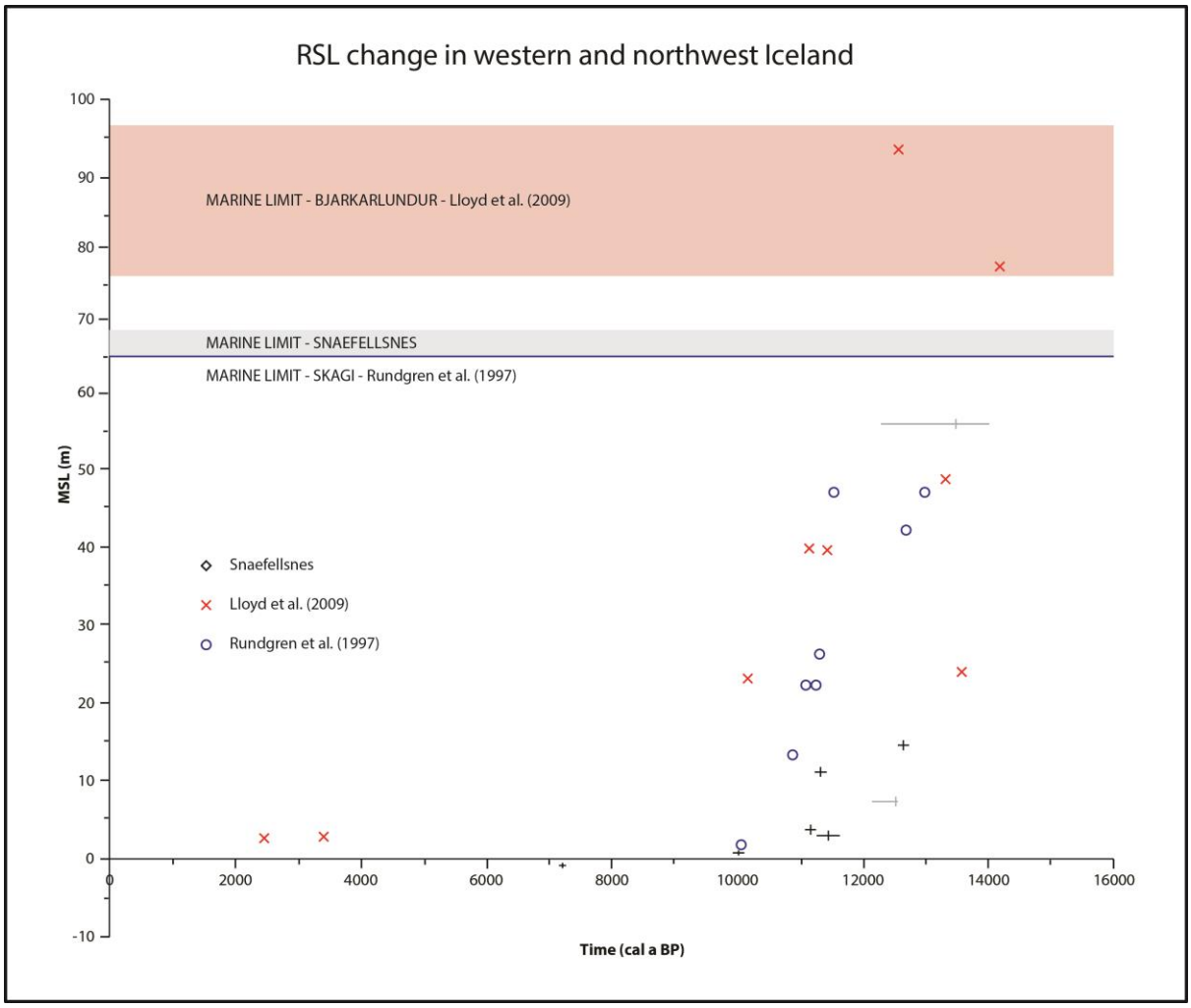

| Site | Lab Code | $^{14}$C age (1σ) BP | Cal. age (2σ) BP | Sill/core altitude (m) | Core Depth (cm) | Indicative Meaning | Mean sea-level (m) |
|---|---|---|---|---|---|---|---|
| **Borgarland 10** | Poz-43545 | 6240 ± 40 | 7148-7259 | 1.8 | 50 | MHWST | -0.2 |
| **Borgarland 11** | SUERC-47976 | 8931 ± 39 | 9915-10097 | 3.1 | 104 | HAT | 0.9 |
| **Skjaldarvatn** | SUERC-47977 | 9973 ± 44 | 11253-11619 | 4.4 | 548 | MHWST-HAT | 2.6 |
| **Þingvallavatn** | Poz-43546 | 9710 ± 60 | 11066-11241 | 5.3 | 505 | MHWST-HAT | 3.2 |
| **Saurar 1** | SUERC-47983 | 10455 ± 43 | 12135-12544 | 9.0 | 332 | MHWST-HAT | 6.8 |
| **Saurar 1** | SUERC-47982 | 10682 ± 44 | 12569-12713 | 9.0 | 336 | N/A | N/A |
| **Helgafellsvatn** | SUERC-47980 | 9493 ± 41 | 10650-10834 | 12.8 | 575 | N/A | N/A |
| **Helgafellsvatn** | SUERC-47981 | 9914 ± 42 | 11224-11408 | 12.8 | 620 | MHWST-HAT | 10.6 |
| **Saurar 3** | Poz-43547 | 10670 ± 60 | 12544-12722 | 16.2 | 808 | MHWST-HAT | 14.1 |
| **Ytra-Bárvatn** | SUERC-47984 | 6972 ± 35 | 7702-7869 | 57.6 | 210 | N/A | N/A |
| **Ytra-Bárvatn** | SUERC-48878 | 16841 ± 76 | 20074-20536 | 57.6 | 468 | MHWST | 56.0 |
| **Ytra-Bárvatn** | BETA-0314 | 20140 ± 60 | 24340-24075 | 57.6 | 440 | HAT | 55.2 |

Table 1: Chronological analyses and sea-level index points from isolation basins and coastal lowland sites within this study. All samples for radiocarbon analysis have undergone a standard acid wash pre-treatment.

**Appendix 1: Lithostratigraphic data from the Stykkishólmur area.**

**Lithostratigraphy of Borgarland 10 (BO10) core**

| Depth (cm) | Sediment description | Tröels-Smith classification |
|---|---|---|
| 0-34 | Mid brown well humified organic material with silt | Th3 Ag1 |
| 34-44 | Brown-grey silt with trace organic material | Ag4 Sh+ |
| 44-56 | Dark grey silt | Ag4 |

**Lithostratigraphy of Borgarland 11 (BO11) core**

| Depth (cm) | Sediment description | Tröels-Smith classification |
|---|---|---|
| 0-109 | Dark brown turfa peat | Th4 |
| 109-117 | Brown-grey silt with trace clay | Ag3 As1 |
| 117-124 | Blue grey silt with gravel and organic material | Ag2 Gmaj1 Sh1 |

**Lithostratigraphy of Skjaldarvatn (SK1) core**

| Depth (cm) | Sediment description | Tröels-Smith classification |
|---|---|---|
| 0-130 | Dark brown turfa peat | Th3 Sh1 |
| 130-144 | Mid brown sphagnum peat | Tb3 Th1 |
| 144-158 | Olive green-grey organic rich silt | Ag3 Sh1 |
| 158-320 | Olive green limus | Ld3 Sh1 |
| 320-546 | Olive green limus with silt | Ld3 Ag1 |
| 546-548 | Tephra | Ag4 |
| 320-548 | Olive green limus with silt | Ld3 Ag1 |
| 548-560 | Blue grey silt | Ag4 As+ |

**Lithostratigraphy of Þingvallavatn (TH1) core**

| Depth (cm) | Sediment description | Tröels-Smith classification |
|---|---|---|
| 0-220 | Mid brown well humified organic material | Sh2 Ld1 Th1 |
| 220-330 | Olive green limus with rootlets and silt | Ld3 Ag1 Th+ |
| 330-420 | Brown organic rich silt | Ag2 Ld2 |
| 420-456 | Olive green-grey organic rich silt | Ag3 Ld1 |
| 456-457 | Tephra | Ag4 |
| 457-479 | Olive green-grey silt | Ag4 Ld+ |
| 479-480 | Tephra | Ag4 |
| 480-492 | Olive green-grey silt | Ag4 Ld+ |
| 492-530 | Dark grey silt with clay | Ag3 As1 Ld+ |

**Lithostratigraphy of Saurar 1 (SA1) core**

| Depth (cm) | Sediment description | Tröels-Smith classification |
|---|---|---|
| 0-200 | Dark brown turfa peat | Th4 |
| 200-290 | Mid brown sphagnum peat | Tb3 Th1 |
| 290-317 | Olive green limus | Ld3 Th1 |
| 317-334 | Olive green limus with silt | Ld2 Ag1 Gmin1 |
| 334-336 | Tephra | Ag4 |
| 336-340 | Olive green limus | Ld4 |

**Lithostratigraphy of Helgafellsvatn (HE1) core**

| Depth (cm) | Sediment description | Tröels-Smith classification |
|---|---|---|
| 0-240 | Dark brown turfa peat with wood and reed fragments | Th2 Dl1 Dg1 |
| 240-400 | Mid brown turfa peat with abundant rootlets | Th4 |
| 400-520 | Olive green silt with mixed organic material and rootlets | Ag2 Ld1 Sh1 |
| 520-578 | Olive green limus with silt and some rootlets | Ld3 Ag1 Sh+ |
| 578-579 | Tephra | Ag4 |
| 579-590 | Olive green limus with silt | Ld2 Ag1 Gmin1 |
| 590-615 | Grey silt | Ag4 |
| 615-616 | Tephra | Ag4 |
| 616-640 | Grey silt | Ag4 As+ |
| 640-655 | Blue grey silt with clay | Ag3 As1 |

**Lithostratigraphy of Saurar 3 (SA3) core**

| Depth (cm) | Sediment description | Tröels-Smith classification |
|---|---|---|
| 0-340 | Dark brown turfa peat | Th4 |
| 340-500 | Olive green limus with turfa peat | Ld3 Th1 |
| 500-810 | Olive green limus | Ld4 Th+ |
| 755-760 | Tephra | Ag4 |
| 760-790 | Olive green limus | Ld4 Ag+ |
| 790-795 | Tephra | Ag4 |
| 795-810 | Olive green limus | Ld4 |
| 810-833 | Dark grey silt | Ag4 Sh+ |
| 833-845 | Dark grey silt with clay | Ag3 As1 |

**Lithostratigraphy of Ytra-Bárvatn (YBR1) core**

| Depth (cm) | Sediment description | Tröels-Smith classification |
|---|---|---|
| 0-90 | Olive green limus | Ld3 Sh1 |
| 90-91 | Tephra | Ag4 |
| 91-210 | Olive green limus | Ld4 |
| 210-211 | Tephra | Ag4 |
| 211-295 | Olive green limus | Ld4 |
| 295-329 | Light brown organic rich limus | Ld3 Sh1 |
| 329-352 | Olive green limus | Ld4 |
| 352-355 | Tephra | Ag4 |
| 355-440 | Olive green limus with trace silt | Ld3 Ag1 |
| 440-480 | Blue grey clay with silt and some organic material | As2 Ag1 Sh1 |